A Ca^{2+}/Calmodulin-Binding Peroxidase from *Euphorbia* Latex: Novel Aspects of Calcium−Hydrogen Peroxide Cross-Talk in the Regulation of Plant Defenses[†,‡]

Anna Mura,[§] Rosaria Medda,[§] Silvia Longu,[§] Giovanni Floris,[§] Andrea C. Rinaldi,[||] and Alessandra Padiglia*[,§]

Departments of Applied Sciences in Biosystems and Biomedical Sciences and Technologies, University of Cagliari, 09042 Monserrato, Cagliari, Italy

Received July 11, 2005; Revised Manuscript Received August 31, 2005

ABSTRACT: Calmodulin (CaM) is a ubiquitous Ca^{2+} sensor found in all eukaryotes, where it participates in the regulation of diverse calcium-dependent physiological processes. In response to fluctuations of the intracellular concentration of Ca^{2+}, CaM binds to a set of unrelated target proteins and modulates their activity. In plants, a growing number of CaM-binding proteins have been identified that apparently do not have a counterpart in animals. Some of these plant-specific Ca^{2+}/CaM-activated proteins are known to tune the interaction between calcium and H_2O_2 in orchestrating plant defenses against biotic and abiotic stresses. We previously characterized a calcium-dependent peroxidase isolated from the latex of the Mediterranean shrub *Euphorbia characias* (ELP) [Medda et al. (2003) *Biochemistry 42*, 8909−8918]. Here we report the cDNA nucleotide sequence of *Euphorbia* latex peroxidase, showing that the derived protein has two distinct amino acid sequences recognized as CaM-binding sites. The cDNA encoding for an *E. characias* CaM was also found and sequenced, and its protein product was detected in the latex. Results obtained from different CaM-binding assays and the determination of steady-state parameters showed unequivocally that ELP is a CaM-binding protein activated by the Ca^{2+}/CaM system. To the best of our knowledge, this is the first example of a peroxidase regulated by this classic signal transduction mechanism. These findings suggest that peroxidase might be another node in the Ca^{2+}/H_2O_2-mediated plant defense system, having both positive and negative effects in regulating H_2O_2 homeostasis.

In plants, as in all eukaryotes, calcium plays a central role as a second messenger in the regulation of a number of physiological processes. Decodification of Ca^{2+} signals is generally devoted to a group of specialized cytosolic proteins that transduce these messages into molecular and cellular responses and integrate calcium signaling into virtually all aspects of plant functioning (*2*−*4*). Among plant Ca^{2+}-sensing proteins, CaM[1] is increasingly appreciated as a critical player. Indeed, since its discovery about 2 decades ago in peanuts and peas (*5*), CaM has been involved in the modulation of diverse cellular and whole plant processes, such as cytoskeleton rearrangement, metabolism, and transcriptional regulation (*6*). Much effort has been dedicated in the last years in identifying downstream target proteins activated by CaM in plants and in understanding their function(s). Some of these studies have recently highlighted the role played by CaM-binding proteins in pollen germination and pollen tube growth (*7*, *8*), in floral development and embryogenesis (*9*, *10*), and in disease resistance and cell death (*11*). Known plant CaM-regulated proteins now include several metabolic enzymes, ion channels, transcription factors, protein kinases/phosphatases, and structural proteins, many of which have no animal counterparts and appear to be unique of plants (*6*, *12*−*14*). Despite these progresses, however, our picture of plant CaM-binding proteins and of their exact positions in Ca^{2+}-mediated signal transduction networks remains largely incomplete.

Class III secreted plant peroxidases are a large family of heme-containing enzymes that oxidize a variety of aromatic molecules in the presence of hydrogen peroxide with the generation of aromatic oxyl radicals and reactive oxygen species (ROS; *15*). Plant peroxidases are found in the cytosol, vacuole, apoplast, or cell wall and participate in crucial physiological events, such as development and growth induction, polymerization of cell wall lignin and suberin precursors, auxin catabolism, wound healing, and defense against pathogen infection. Although peroxidases are generally reported to participate in the activation of plant defense responses mainly through their contribution to the oxidative burst in which levels of ROS (particularly superoxide and H_2O_2) rapidly increase, an expanded scenario is emerging in which these proteins might interact in more complex ways

[†] This study was partially supported by FIRB (Fondo per gli Investimenti della Ricerca di Base) funds obtained from the Italian Ministry of Education, University and Research.

[‡] The sequences reported in this paper have been deposited in the GenBank database (*Euphorbia characias* peroxidase, accession number AY586601; *E. characias* calmodulin, accession number AY297816).

* To whom correspondence should be addressed. Tel: +39 070 6754515. Fax: +39 070 6754523. E-mail: padiglia@unica.it.

[§] Department of Applied Sciences in Biosystems, University of Cagliari.

[||] Department of Biomedical Sciences and Technologies, University of Cagliari.

[1] Abbreviations: ABTS, 2,2′-azinobis(3-ethylbenzothiazoline-6-sulfonic acid); BBCaM, bovine brain calmodulin; CaM, calmodulin; ECaM, *Euphorbia* calmodulin cDNA; ELCaM, *Euphorbia* latex calmodulin (protein); EP, *Euphorbia* peroxidase cDNA; ELP, *Euphorbia* latex peroxidase (protein); MOPS, 3-(*N*-morpholino)propanesulfonic acid; RT-PCR, reverse transcription polymerase chain reaction; SDS−PAGE, sodium dodecyl sulfate−polyacrylamide gel electrophoresis.

10.1021/bi0513251 CCC: $30.25
Published on Web 10/05/2005

with defense-related compounds and systems. Peroxidases have been recently indicated as components of the salicylic acid signaling pathway, a mechanism responsible for eliciting plant responses that lead to local and systemic disease resistance after pathogen attack (*16*, *17*). Furthermore, peroxidases are clearly implicated in the homeostasis of hydrogen peroxide which, besides being the key component of the oxidative burst, is believed to act as a second messenger for the induction of plant defensive genes (*18*, *19*), a messenger whose production/degradation is finely tuned by calcium (refs *20* and *21* and references cited therein).

We have previously reported on the purification and characterization of a peroxidase from the latex of the Mediterranean shrub *Euphorbia characias* (*1*). Contained in the laticifer-specialized cells forming vessel-like structures that permeate various aerial tissues of about 20 plant families and present in all Euphorbiaceae (*22*, *23*) latex is a milky sap with a complex composition that includes alkaloids, terpenoid compounds, and a number of enzymes (*24*) that collectively are believed to provide an important contribution to plant defense mechanisms by repelling and killing phytopathogens and sealing wounded areas (*25*). *Euphorbia* latex peroxidase (ELP) was found to contain one ferric iron−protoporphyrin IX as the heme prosthetic group plus 1 mol of endogenous calcium/mol of enzyme, and its catalytic efficiency was enhanced by 3 orders of magnitude by an excess of Ca^{2+} ions in vitro. In this study, we isolated and sequenced the ELP cDNA, showing that the mature protein harbors two distinct CaM-binding sites. ELP−CaM interaction was also determined experimentally and by computer-assisted prediction methods. Subsequently, the presence of CaM in the latex was demonstrated, and the encoding cDNA was also found and sequenced. Finally, we showed that Ca^{2+}/CaM enhanced ELP activity. On the basis of these results we propose that Ca^{2+}/CaM participates in the regulation of *Euphorbia* latex peroxidase activity and, presumably, in the associated plant defense mechanisms. To the best of our knowledge, this is the first report of a CaM-binding peroxidase.

MATERIALS AND METHODS

Plant Material, Enzymes, and Chemicals. Horseradish peroxidase (HRP), bovine brain calmodulin (BBCaM), and 2,2′-azinobis(3-ethylbenzothiazoline-6-sulfonic acid) (ABTS) were purchased from Sigma (St. Louis, MO). *o*-Dianisidine and hydrogen peroxide were from Merck (Darmstadt, Germany). An $\epsilon_{240} = 43.6\ M^{-1}\ cm^{-1}$ was used to determine H_2O_2 concentration. All chemicals were obtained as pure commercial products and used without further purification. *E. characias* latex drawn from cut branches and young leaves was collected in the four seasons at several locations in southern Sardinia (Italy), frozen, and stored at −20 °C until use. *Euphorbia* latex peroxidase (ELP; RZ value $A_{403}/A_{280} = 2.7$) was purified from crude latex as previously described (*1*). ELP concentration was estimated using an $\epsilon_{401} = 130.7\ mM^{-1}\ cm^{-1}$ (*1*). Calcium content was measured by atomic absorption using a Unicam 969 AA spectrometer Solar (Bournemouth, Dorset, U.K.). The heme content was determined from the absorption spectra of the oxidized and reduced forms of the pyridine hemochromogen derivative, assuming a differential absorption coefficient of $\Delta\epsilon_{541}$ (for the dithionite-reduced enzyme) − $\Delta\epsilon_{557}$ (for the ferricyanide-oxidized enzyme) = $20.7\ mM^{-1}\ cm^{-1}$ (*26*).

Peroxidase Activity. Activity measurements were performed in 100 mM MOPS buffer, pH 6.5, at 25 °C, using hydrogen peroxide and the reducing substrate ABTS by following the increase in absorbance at 415 nm resulting from the formation of the ABTS cation radical product ($\epsilon_{415} = 36\ mM^{-1}\ cm^{-1}$). Activity was calculated in standard enzyme units (μmol min^{-1} mg^{-1}), and catalytic center activity (k_{cat}) was defined as (mol of substrate consumed)/(mol of active sites) in 1 s. The value of K_M for ELP using varying reducing substrate concentrations at a saturating concentration of hydrogen peroxide (25 mM) or varying concentrations of hydrogen peroxide at a saturating concentration of reducing substrate (10 mM ABTS) was calculated from double reciprocal plots by Michaelis−Menten analysis. k_{cat} values were compared to that obtained for HRP. The effects of Ca^{2+} ions on ELP activity were examined in buffers with or without $CaCl_2$, and BBCaM was included in the reaction mixture at concentrations indicated in the figure legends.

Western Blot Analysis of Euphorbia Calmodulin. Western blot was used to verify the presence of ELCaM in the crude latex and during the purification process of ELP. Protein fractions from crude latex and from different ELP purification steps were resolved by electrophoresis, transferred onto nitrocellulose, and immunolabeled with a monoclonal mouse anti-CaM clone 6D4 IgG (Sigma) and then with a secondary rabbit anti-mouse IgG HRP-conjugated antibody (Sigma), according to the manufacturer's recommendations. Detection was performed with a ProteoQwest colorimetric western blotting kit TMB substrate (Sigma).

Isolation of RNA and RT-PCR. Total RNA was isolated from 0.5 g of liquid N_2 frozen *Euphorbia* young leaf powder using the RNacqueous isolation kit (Ambion, Austin, TX) and the plant isolation aid reagent (Ambion) to increase the RNA yield, according to the manufacturer's instructions. For RNA extraction from latex, *E. characias* branches were sliced, and the fresh latex (≈5 mL) flowed directly into a tube containing 20 mL of 2 × RNA extraction buffer (0.1 M Tris-HCl, 0.3 M LiCl, 0.01 M EDTA, 10% SDS, pH 9.5) with 5 mL of RNAlater solution (Sigma) to stabilize and protect RNA. The latex solution was mixed and centrifuged at 8000*g* for 15 min at 20 °C. The supernatant fraction was processed using TRI Reagent RNA isolation reagent (Sigma) according to the manufacturer's instructions. The quality of purified RNA from both leaves and latex was verified by gel electrophoresis using 1% denaturing agarose gel stained with ethidium bromide and by the absorbance spectrum from 220 to 300 nm. To obtain cDNAs, *Euphorbia* RNAs from latex and leaf were reverse transcribed with an oligo(dT) primer using an enhanced avian myeloblastosis virus reverse transcriptase enzyme (Sigma). All PCR and nucleic acid blotting experiments described below were carried out using both latex and leaf cDNA.

Euphorbia Calmodulin and Peroxidase cDNAs. Amplification by PCR with Hybrid Primers. Degenerate oligonucleotide primers were designed using the consensus degenerate hybrid oligonucleotide primer (CODEHOP) strategy (*27*), starting from the alignment of multiple calmodulin and peroxidase protein sequences from different plant sources. Five sequences for peroxidase and six for calmodulin were chosen from the GenBank database and aligned using

ClustalW (http://www.ebi.ac.uk/clustalw) and then cut into blocks using the Block Marker software (http://blocks.fhcrc.org/blocks/). Primers were designed using the default parameters at the CODEHOP server (http://blocks.fhcrc.org/codehop.html), and sets of sense and antisense primers were selected for each protein. For *Euphorbia* peroxidase (EP) the primers 5′-CGGCTGCACTTCCACgaytgyttygt-3′ and 5′-AGGTCCACGTAGtayttrttrtc-3′ were used in the sense and antisense orientation, respectively. For *Euphorbia* calmodulin (ECaM) one sense primer, 5′-GGCCTTCTCCCTGTTCgayaargaygg-3′, and three antisense primers, 3′-tytacttyctrtGGCTGAGGCTCCTCCTC-5′, 3′-ctrgtyttrccGAAGTAGAGGCGGC-5′, and 3′-ctrctytacyaGGCCCTCCGGCTG-5′, were employed (see Supporting Information). For each primer, the consensus clamp is given in upper case, whereas the degenerate core is in lower case: y = [C,T]; r = [A,G]. In the case of ECaM, the sense primer was used in different PCR experiments in combination with each of the three selected antisense primers (see Supporting Information). For both EP and ECaM, PCR was performed in a solution containing 1.5 mM $MgCl_2$, 100 mM Tris-HCl, pH 8.3, 50 mM KCl, 200 mM dNTP mix, 1 mM sense primer, 1 mM antisense primer, 1 mg of *Euphorbia* cDNA, and 1−3 units of Jump Start AccuTaq LA DNA polymerase mix (Sigma). Thermal cycles of amplification were carried out in a DNA thermal cycler from Perkin-Elmer (Norwalk, CT) and in a Personal Eppendorf Mastercycler (Eppendorf, Hamburg, Germany) using slightly different programs for EP and ECaM. CODEHOP PCR products of each protein were identified by Southern blot using homologous cDNA fragments as probes and standard procedures.

Rapid Amplification of cDNA Ends (RACE). Rapid amplification of the 5′ and 3′ ends was done as reported (*28*), using antisense-specific primers and the anchor primer provided in the RACE kit (Roche Diagnostics, Mannheim, Germany). To perform 5′ RACE for ECaM, the antisense-specific primer 5′-TGTCATCACATGACGAAGCTCGGCAGC-3′ was used in a reverse transcription reaction with 2 mg of *E. characias* total RNA. The first strand cDNA was purified from unincorporated nucleotides and primers by the High Pure PCR purification kit (Roche Diagnostics). A homopolymeric tail was added to the 3′ end of RT-PCR products, and the obtained cDNA was amplified by PCR using the nested antisense-specific primer 5′-GCCATCAGATTAAGGAACTCTGGGAA-3′ and the oligo(dT)-anchor primer provided in the RACE kit, according to the protocol supplied. For 3′ RACE, the first strand cDNA was obtained using the oligo(dT)-anchor primer and amplified using the sense-specific primer 5′-GGAGGAGCTCAAGGAAGCTTTCCGTG-3′ or 5′-CTCGGCGAGAAACTCACTGATGAGGAGG-3′ and the antisense PCR anchor primer provided in the RACE kit. PCR reactions were performed using 1−3 units of Jump Start AccuTaq LA DNA polymerase mix (Sigma) under different experimental conditions. For 5′ RACE concerning EP, the antisense-specific primer 5′-GAGCAGGAGACGACGGGGCCACACTCC-3′ was used in a reverse transcription reaction as reported for ECaM. The obtained cDNA was amplified by PCR using the nested antisense-specific primer 5′-GCTCACTGGGTCCACCCGCTGACCC-3′ and the oligo(dT)-anchor primer provided in the RACE kit. For 3′ RACE, the first strand cDNA was obtained using the oligo(dT)-anchor primer and amplified using the 5′ sense-specific primer 5′-GCCCCAACGTGAACACGGAGAACTC-3′ and the antisense PCR anchor primer provided in the RACE kit. PCR reactions were performed as described above for ECaM.

cDNA Sequencing and Analysis. cDNA sequencing was performed by MWG Biotech (Ebersberg, Germany). Nucleotide and deduced amino acid sequence analyses were performed either with the OMIGA version 2.0 software (Oxford Molecular, Madison, WI) or with programs accessible on the Internet. Translation of nucleotide sequences was performed using OMIGA or the ExPASy translate routine software (http://ca.expasy.org/). Similarities were analyzed with the advanced BLAST algorithm, available at the National Center for Biotechnology Information website (http://www.ncbi.nlm.nih.gov/), and with the FASTA algorithm version 3.0 from the European Bioinformatics Institute website (http://www.ebi.ac.uk/fasta33/index.htlm). Sequences were aligned with ClustalW.

Southern Blot Genomic DNA Analysis. DNA was obtained from young *E. characias* leaves using a Plant DNA isolation kit (Roche Diagnostics). *Euphorbia* genomic DNA (10 μg per assay) was digested with 10−20 units each of *Eco*RI, *Hin*dIII, and *Bam*HI (Sigma) in the buffer recommended by the manufacturer at 37 °C for 4 h. Digested DNAs were electrophoresed in a 1% agarose gel and blotted to Hybond nylon membranes (Amersham Biosciences, Buckinghamshire, U.K.). Filter membranes were then hybridized with full-length EP or ECaM cDNA, from latex or from leaves, as a probe.

Northern Blot Analysis. Total RNA samples (10 μg) were dried in a Speedvac, dissolved in 20 μL of RNA sample loading buffer (Sigma), and heated to 60 °C for 10 min. The samples were snap-cooled on ice and loaded onto a 1.2% agarose and 1 × MOPS (0.2 M MOPS, 10 mM EDTA, 0.5 M sodium acetate, pH 7) gel, containing 0.66 M formaldehyde and ethidium bromide together with 0.3−6.9 kilobase RNA marker (Roche Diagnostics, Mannheim, Germany). The gel was run at 5 V/cm in 1 M MOPS buffer, and then RNA was transferred overnight to a positively charged nylon membrane (Roche Diagnostics) by capillary blotting in 20 × SSC buffer (3 M NaCl, 0.3 M trisodium citrate, pH 7.0). The blot was baked for 30 min at 120 °C. The membrane was then hybridized with a full-length ECaM or EP as a probe. The probe labeling and hybridization process were made as described in the Southern Blot Genomic DNA Analysis section.

cDNA Blotting Analysis. cDNA blotting was performed to confirm the results obtained with northern blot analysis. This method resolves several problems associated with northern blotting and is especially efficient when applied to recalcitrant plant material like *E. characias* tissues (*29*). The cDNAs obtained from total RNA samples (5 μg) reverse-transcribed were run on a 1.2% agarose gel for 10 h at 18 V and then stained in ethidium bromide. After two washes in both denaturing (0.5 M NaOH, 1.5 M NaCl) and neutralizing (0.5 M Tris-HCl, 3 M NaCl, pH 7.5) buffers, the gel was transferred overnight to a positively charged nylon membrane (Roche Diagnostics) by capillary blotting in 20 × SSC buffer. The filter membrane was hybridized with a full-length ECaM or EP cDNA as a probe as described in the Southern Blot section.

Calmodulin-Binding Assays. Calmodulin-binding assays were performed as follows:

(i) Affinity Chromatography on Calmodulin−Sepharose. Samples of ELP and ELAO were applied to a calmodulin−Sepharose column (Amersham Pharmacia Biotech, Uppsala, Sweden) equilibrated with a binding buffer composed of 50 mM Tris-HCl (pH 7.4) and 5 mM $CaCl_2$ (buffer A). After the column was washed with buffer B composed as (A) but containing 1 M NaCl in order to remove nonspecifically bound proteins, ELP was eluted from the column with buffer C containing 25 mM Tris-HCl buffer, pH 7.4, containing 2 mM EGTA, a calcium chelating agent. The amount of protein eluted was estimated by Bradford's method with a protein assay kit (Bio-Rad, Milan, Italy). In particular, the presence of ELP was detected spectrophometrically at 401 nm using $\epsilon_{401} = 130.7\ mM^{-1}\ cm^{-1}$ (*1*).

(ii) Analytical Polyacrylamide Gel Electrophoresis (PAGE). Purified ELP was incubated with various amounts of bovine brain calmodulin in the presence and absence of Ca^{2+} ions. Then PAGE was performed under standard methods. The gel was stained with Coomassie blue, and protein bands with peroxidase activity were detected by staining the gel after the electrophoretic run in buffer containing *o*-dianisidine and hydrogen peroxide.

RESULTS

Isolation of Peroxidase cDNA from Euphorbia Latex. To get insight into the role of a calcium-dependent peroxidase that we previously characterized after isolation from *Euphorbia* latex (*1*), we cloned the corresponding cDNA from *Euphorbia* RNA by RT-PCR as described above. The ELP cDNA sequence was determined for both strands using a progressive primer design strategy. The complete cDNA contains an open reading frame (ORF) of 1044 bp that extends from the ATG codon at positions 38−40 to the termination codon at position 1081 (Figure 1). The 3′-untranslated (3′ UTR) region includes a putative polyadenylation signal AATAAA located 259 bp upstream of the polyadenylation [poly(A)] tail. The ELP gene encodes a protein of 347 amino acids (Figure 1). The protein isolated from *Euphorbia* latex is not accessible to N-terminal sequencing because of a pyroglutamate block, a situation that is common in plant peroxidases, but its N-terminal amino acid was previously identified as glutamine (*1*). The cDNA sequence reveals that this residue does not initiate the ORF, but it follows a 22 aa leader sequence with characteristics of a secretion signal peptide (Figure 1). The deduced amino acid sequence of ELP shares significant identity (52−64%) and similarity (68−78%) with secretory peroxidases from different plant sources, including *Nicotiana tabacum*, *Phaseolus vulgaris*, *Linum usitatissimum*, *Arabidopsis thaliana*, and *Glycine max* (see Supporting Information).

Determination of the ELP gene sequence allowed for a refined characterization of the protein with respect to other interesting features not previously elucidated in full. In particular, availability of the ELP primary structure permitted to draw a coherent representation of the calcium ion binding sites. As horseradish peroxidase (HRP) and other secretory plant peroxidases, ELP has two calcium-binding sites, respectively proximal and distal to the heme. The role of calcium ions in plant peroxidase has been explored for years, and calcium is currently thought to be required for the stability of the enzyme and for regulating the heme pocket structural and catalytic properties (*30*, *31*). In ELP, the proximal Ca^{2+} ion is strongly bound and is essential for maintaining the protein structure around the heme environment, while, at variance with other plant peroxidases, the distal Ca^{2+} is in a low-affinity binding site but is necessary for expression of full enzyme activity (*1*). The ELP sequence harbors all of the plant peroxidases' highly conserved amino acid residues coordinated to the heme and calcium ions (Figure 1), and the local structure of the proximal and distal Ca^{2+}-binding sites can now be hypothesized (Figure 2) in comparison with that known for HRP (*30*, *31*).

Further information was also gathered on the ELP glycosylation and cysteine residue/disulfide bridge patterns. The protein was previously shown to have an approximate 15% carbohydrate content, with a shift in the M_r from 46 to 39 kDa after deglycosylation, as measured by SDS−PAGE (*1*). The ELP predicted sequence now revealed six potential N-glycosylation sites (N-X-S/T) at amino acids 64−66 (NGS), 78−80 (NLS), 142−144 (NAT), 154−156 (NVT), 220−222 (NST), and 278−280 (NQT) (Figure 1). Eight Cys residues are present at positions 19, 42, 47, 100, 106, 186, 213, and 310; thus four disulfide bridges are expected in the native protein. After incubation with 1.6 mM 5,5′-dithiobis(2-nitrobenzoic acid) or 7-fluoro-4-nitrobenz-2-oxa-1,3-diazole at 30 °C for 60 min, 8 mol of cysteine residues/mol of enzyme could be titrated in the presence of 6 M guanidine hydrochloride. In the native enzyme, no detectable decrease in peroxidase activity was recorded in the presence of cysteine reagents, and no sulfhydryl groups were titrable.

Euphorbia Peroxidase Is a CaM-Binding Protein. The characterization of ELP as a CaM-binding protein was also achieved. (i) Analysis of the predicted amino acid sequence of ELP for putative CaM-binding sites was made with the tools provided by the web-based Calmodulin Target Database (http://calcium.uhnres.utoronto.ca/ctdb). In this method, sequences are analyzed for features such as hydropathy, α-helical propensity, residue charge, and hydrophobic residue content, and a normalized score (0−9) is attributed on the basis of these criteria. A string of high values indicates the location of a putative binding site (*32*). Our search revealed the presence of a putative CaM-binding domain between residues 26−39 of ELP, a 14 aa sequence (IQKELKKLFKKDVE) with the characteristics of a IQ-like motif (Figures 1 and 3). In addition, a related motif for CaM binding, termed 1-8-14, was spotted between residues 79 and 92 (LSLRKQAFKIVNDL; Figures 1 and 3). IQ motif and related sequences are present, often in multiple copies, in diverse families of CaM-binding proteins such as myosins, neuromodulin, neurogranin, and brain-specific polypeptide PEP-19 and have been shown to bind CaM both in the presence and in the absence of calcium, depending on the occurrence of particular residues in the sequence (*33*−*36*). The 1-8-14 motif makes a subclass of the larger 1-14 motif family, a group of sequences characterized by the presence of two or more bulky hydrophobic residues spaced by a variable number of amino acids (*37*). These sequences bind to CaM primarily in the presence of calcium. The CaM-binding potential of the identified IQ-like and 1-8-14 motifs in the ELP sequence was also verified by computer-assisted prediction of their ability to form a basic, amphiphilic α-helix and

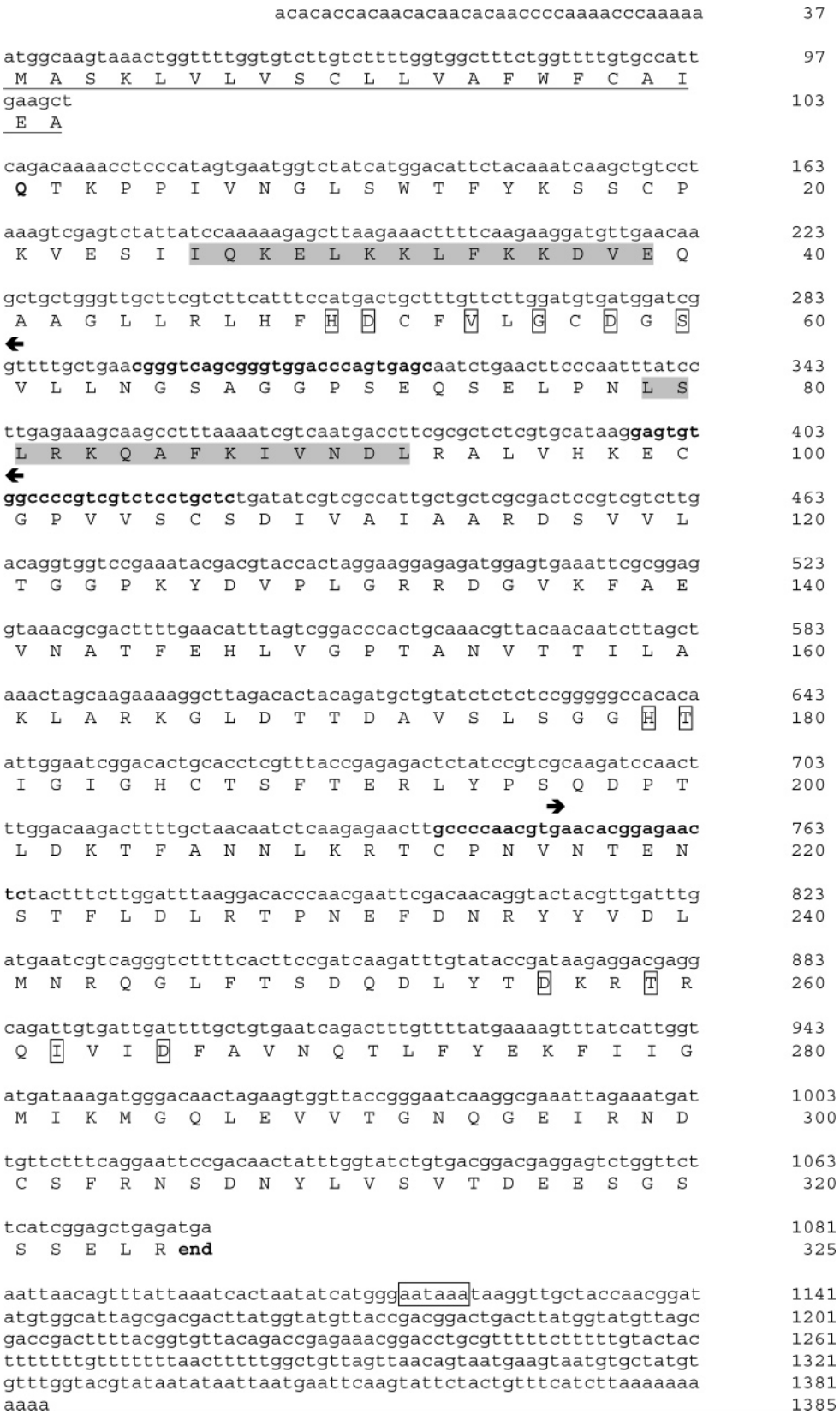

FIGURE 1: Nucleotide and deduced amino acid sequence of *E. characias* peroxidase. The nucleotide sequence is numbered in the 5′ to 3′ direction. The terminal tga codon is indicated by end. The polyadenylation signal aataaa (nt 1116−1121) is boxed. The signal peptide portion of the protein is underlined. Q corresponds to the N-terminal residue in mature peroxidase. Specific sense (→) and antisense (←) primers used in RACE experiments are in bold. The predicted CaM-binding IQ-like motif (peptide 26−39) and 1-8-14 motif (peptide 79−92) are shown in gray. The deduced heme distal and proximal histidine residues, His_{50} and His_{179}, and the Ca^{2+} ligands at the distal (Asp_{51}, Val_{54}, Gly_{56}, Asp_{58}, Ser_{60}) and proximal (Thr_{180}, Asp_{256}, Thr_{259}, Ile_{262}, Asp_{265}) metal-binding sites are boxed (see Figure 2 for more structural details). These residues are highly conserved in all plant peroxidases.

by calculating the relevant hydrophobicity and hydrophobic moment. Interaction between CaM and target proteins is known to be mainly hydrophobic in nature and to require specific binding of CaM to short basic peptides in target

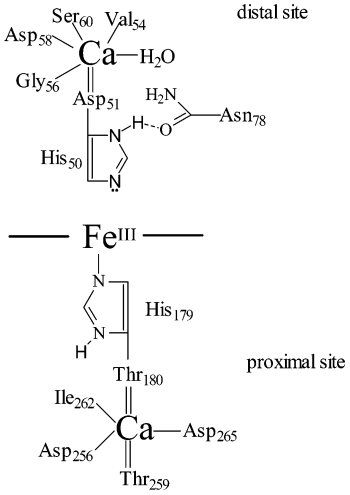

FIGURE 2: Structure of the calcium-binding sites in ELP. The proximal and distal calcium-binding sites in *Euphorbia* latex peroxidase have been hypothesized from analysis of the protein's sequence and comparison to structural features of HRP (*30*, *31*). Only the direct coordination environment is shown, but several other amino acids close to the calcium ions are also highly conserved and are probably important for maintaining the correct geometry of the binding sites and of the heme pocket. Both Ca^{2+} ions are seven coordinated. In ELP, the distal Ca^{2+} is loosely bound, but it is necessary for expression of the full enzyme's activity (*1*).

sequences, these peptides having a net propensity to form amphiphilic α-helical structures (*12*, *38*). The helical wheel projection, propensity for α-helix formation, mean residue hydrophobicity (H), and mean hydrophobic moment (μ) for the ELP putative CaM-binding peptides are given in Figure 3. The potential for these cationic peptides to be structured as an amphipathic α-helix is manifest, and the calculated H and μ values and other parameters fit those reported for the IQ and 1-14 classes, respectively (http://calcium.uhnres.utoronto.ca/ctdb). (ii) ELP was found to tightly bind to a CaM−Sepharose column in the presence of calcium and eluted with EGTA, whereas the protein did not bind to a column equilibrated in the absence of calcium or in the contemporary presence of calcium and EGTA, indicating that CaM binding to ELP is Ca^{2+} dependent (data not shown).

Reaction of ELP with Hydrogen Peroxide and Reducing Substrates: Kinetic Parameters in the Absence and in the Presence of Calcium Ions. ELP activity was tested in 100 mM MOPS buffer, pH 6.5, using ABTS as substrate. The value of K_M for ABTS at a saturating concentrations of hydrogen peroxide was shown to be 1.25 mM whereas the K_M for hydrogen peroxide at a saturating concentration of ABTS was calculated to be 3 mM (not shown). When native ELP was incubated for 10 min in the presence of Ca^{2+}, an activation was observed (Figure 4) which showed a maximum at 10 mM Ca^{2+} ion concentration (40-fold) with a drastic increase of k_{cat}. Under these conditions, calcium is thought to saturate the distal low-affinity binding site, converting the enzyme from an almost inactive form, with only the proximal Ca^{2+} ion bound, to a fully active form with both the proximal and distal calcium ions in situ (*1*). More in detail, Ca^{2+} binding to the low-affinity site is believed to induce the reorientation of the heme distal His, favoring its action as a general acid−base catalyst in the peroxidase reaction mechanism.

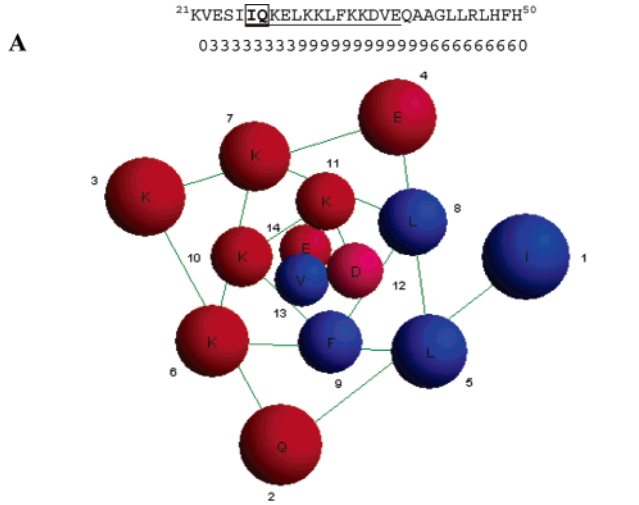

H = -1.029; μ = 1.721. Average propensity for α-helix formation = 1.188

H = 0.079; μ = 1.584. Average propensity for α-helix formation = 1.084

FIGURE 3: Prediction of CaM-binding sites in ELP. The full amino acid sequence was analyzed to predict CaM-binding sites using the CaM Target Database (http://calcium.uhnres.utoronto.ca/ctdb). Analysis revealed two putative CaM-binding sequences, namely, an IQ-like motif (A) and a 1-8-14 motif (B). The numbers under the sequences indicate normalized scores (0−9) based on the evaluation criteria for CaM-binding sites (see *Euphorbia* Peroxidase Is a CaM-Binding Protein for details). The predicted IQ-like motif (peptide 26−39) and 1-8-14 motif (peptide 79−92) are underlined. Helical wheel diagrams of the predicted CaM-binding peptides are also shown. Charged or hydrophilic residues are shaded in nuances of red-violet; hydrophobic residues are in blue. Mean residue hydrophobicity (H) and hydrophobic moment (μ) were calculated using the Kyte−Doolittle scale of hydrophobicity (*50*). The average propensity for α-helix formation was calculated using the Chou−Fasman values (*51*).

E. characias latex contains free calcium ions as determined by atomic absorption, and the Ca^{2+} content varies from 2.1 (±0.1) mM in the winter to 3.5 (±0.15) mM in the summer. Thus we can conclude that the activation of ELP due to the free calcium in the latex can oscillate between 18- and 24-fold. Crude latex was shown to contain a mean of 26 mg/mL total proteins, as determined by Bradford's method, and ELP activity was 8 nkat/mL (not shown). When ELP activity was detected in the latex in the presence of 10 mM Ca^{2+} ions, we showed a 12-fold increase in activity, about three

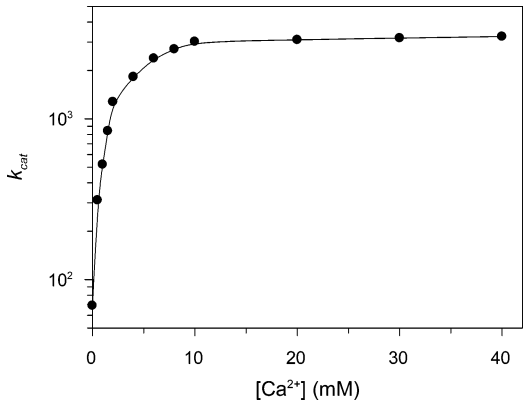

FIGURE 4: Response of *Euphorbia* peroxidase activity to Ca^{2+}. ELP activity in 100 mM MOPS, pH 6.5, and in the presence of calcium ions. The continuous curve represents the theoretical binding isotherm fit to the data.

times less than that obtained in successive steps of ELP purification (*1*). It may be indicative of a higher basal peroxidase activity of the protein when in the latex environment. Since we used for detection of ELP activity 1 mL of MOPS containing 50 μL of a 200-fold diluted latex, it corresponded to 2×10^{-3} nkat/mL of ELP and 0.88 μM calcium ions. This amount of calcium did not perturb per se ELP activity when added to samples of purified enzyme (Figure 4). Samples of latex were then dialyzed in MOPS buffer, pH 6.5, in the presence of 0.4 mM EGTA for 12 h and then dialyzed exhaustively in MOPS buffer without EGTA. After this treatment, a lower basal activity was recorded in ELPsamples but a 40-fold activation of ELP activity was observed in the presence of 10 mM calcium ions. The loss of the strongly bound proximal calcium ion after treatment with EGTA can be excluded, since this can only be achieved by incubating the enzyme in 100 mM Tris-HCl buffer, pH 7.2, for 18 h at 25 °C with 6 M guanidine hydrochloride and 10 mM EGTA, as previously shown (*1*). Altogether, these results suggest the presence of an activating factor in the latex, and we believe it can be safely assumed that it might be calmodulin.

Isolation of Calmodulin cDNA from Euphorbia. As detailed, the ELP sequence contains a CaM-binding IQ-like motif and a related motif termed 1-8-14 (Figure 1). Starting from this evidence, we thus looked for, found, and cloned a *Euphorbia* cDNA coding for a CaM protein. We later spotted this protein as expressed in the plant latex (see below) and therefore named it *Euphorbia* latex calmodulin (ELCaM). The ELCaM cDNA contains an ORF of 447 bp which can be translated to a protein sequence of 149 amino acids (Figure 5). The ATG codon at nucleotides 71−74 most probably represents the protein translation initiation site. The 3′-untranslated region includes a putative polyadenylation signal AATAAA located 26 bp upstream of the poly(A) tail. The calculated molecular mass for the predicted protein is 16850 kDa, with a p*I* of 4.1. Not surprisingly, the ELCaM amino acid sequence shows a very high degree of identity (91−100%) and similarity (99−100%) to CaMs isolated from several other higher plants, including *Prunus avium*, *Elaeis*

```
aaggtccggcatagaaactcaaatcaaagaggaagaaacaccgattctccttttctctct     60
ctaaacaact                                                       70

atggcagatcaactcacagacgatcagatctctgagtttaaggaagctttcagcctcttc    130
 M  A  D  Q  L  T  D  D  Q  I  S  E  F  K  E  A  F  S  L  F     20

gacaaggatggcgatggttgtatcactactaaggaactcgggactgtgatgagatcgttg    190
 D  K  D  G  D  G  C  I  T  T  K  E  L  G  T  V  M  R  S  L     40

ggtcagaatccaactgaagcagagctacaagacatgataaacgaggttgatgctgatgga    250
 G  Q  N  P  T  E  A  E  L  Q  D  M  I  N  E  V  D  A  D  G     60
                        ←
aatggcaccatcgattcccagagttccttaatctgatggccgcaagatgaaggacact      310
 N  G  T  I  D  F  P  E  F  L  N  L  M  A  R  K  M  K  D  T     80
                     →
gattctgaggaggagctcaaggaagctttccgtgttttgacaaggatcagaatggtttc     370
 D  S  E  E  E  L  K  E  A  F  R  V  F  D  K  D  Q  N  G  F    100
                  ←                          →
atttctgctgccgagcttcgtcatgtgatgacaaatctcggcgagaaactcactgatgag    430
 I  S  A  A  E  L  R  H  V  M  T  N  L  G  E  K  L  T  D  E    120

gaggttgatgagatgatccgtgaggctgatgttgatggcgatggtcagatcaactacgaa    490
 E  V  D  E  M  I  R  E  A  D  V  D  G  D  G  Q  I  N  Y  E    140

gagtttgtgaaagtcatgatggccaagtga                                  520
 E  F  V  K  V  M  M  A  K  end                                 149

aggtcacggagcatcatctagagtatcaaccactactagtccaagagtagtacatgacgt    580
cttaggataaaacagattcgtgaatgctttttcctctgatctcttctttttctccctttgt    640
attttcgcctgccttctccttcctctctcgttgtatattttcactatttccctttttctt    700
atgtgattaaacgaaaactatattacttgttcacactgaggaataaatctttctaagttg    760
tgccttcaaaaaaaaaaaaaaaaaaaaaaaa                                 792
```

FIGURE 5: Nucleotide and deduced amino acid sequence of the *E. characias* CaM. The nucleotide sequence is numbered in the 5′ to 3′ direction. The termination tga codon is indicated by end. The polyadenylation signal AATAAA (nt 742−747) is boxed. M corresponds to the N-terminal residue in mature CaM. The four EF-hand domains are underlined, and the Ca^{2+}-binding amino acid residues are boxed. Specific sense (→) and antisense (←) primers used in RACE experiments are in bold.

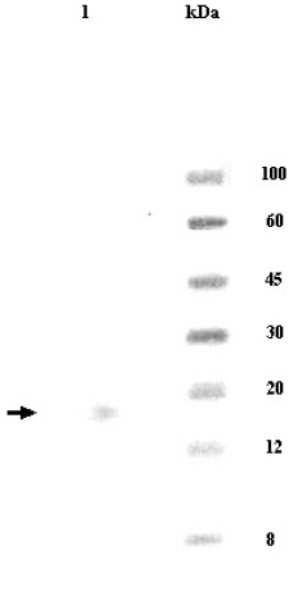

FIGURE 6: *Euphorbia* CaM expression in the latex. Protein samples from *Euphorbia* latex were separated by SDS−PAGE, transferred to nitrocellulose, and immunoblotted using a monoclonal mouse anti-CaM clone 6D4 IgG and a secondary rabbit anti-mouse IgG HRP-conjugated antibody. A single reactive band was detected (lane 1).

guineensis, *Medicago truncatula*, *Pisum sativum*, *P. vulgaris*, and *N. tabacum* (see Supporting Information).

CaM Is Expressed in Euphorbia Latex. To test whether CaM was present in *Euphorbia* latex, the crude latex was immunoblotted using antibodies specific for the CaM-binding domain. A single reactive band was detected (Figure 6), demonstrating that *Euphorbia* CaM is expressed in the latex, where it coexists with ELP. Attempts were also made to verify whether and to which extent ELCaM remains associated to ELP during the latter protein's purification process from the latex, but apparently ELCaM is lost at the first step of ELP purification and proved itself particularly recalcitrant to isolation in pure form.

ELP Activity in the Absence and in the Presence of Bovine Brain Calmodulin and Calcium Ions. To study the significance of Ca^{2+}/CaM binding to *Euphorbia* latex peroxidase, the catalytic activity of purified ELP was measured in the presence and absence of Ca^{2+} ions and bovine brain CaM (BBCaM). We used BBCaM for its very high amino acid sequence identity (≈90%) to ELCaM (Figure 7). These experiments were carried out using HRP as a reference for peroxidase activity. Addition of BBCaM alone was insufficient to activate ELP, whereas in the presence of both calcium and calmodulin the enzyme displayed a marked increase in activity (Figure 8 and Table 1). Not surprisingly, no difference in catalytic activity was observed for HRP at any Ca^{2+} and/or BBCaM combination (Table 2). Ca^{2+}/BBCaM is thus able to stimulate ELP activity, elevating the very poor k_{cat} of the native enzyme (with only the proximal calcium ion bound) to a value comparable to that of HRP. Although ELCaM displays an elevated sequence identity to BBCaM, it is presumable that ELCaM, by binding ELP with greater affinity and specificity with respect to BBCaM, might likely cause an even greater enzyme activation than that seen with its bovine homologue. Finally, when samples of pure *Euphorbia* peroxidase were incubated with BBCaM in the absence and in the presence of 300 μM Ca^{2+} ions and electrophoresed under nondenaturing conditions, activity staining revealed ELP bands only when both BBCaM and calcium ions were present in the reaction mixture (Figure 9).

Table 1: Kinetic Parameters of *Euphorbia* Latex Peroxidase in the Presence and Absence of Ca^{2+} Ions and in the Presence and Absence of Bovine Brain Calmodulin (0.3 μM)[a]

	ELP	ELP−Ca^{2+} [d]	ELP−BBCaM[e]
K_M(ABTS)[b] (mM)	1.3 ± 0.12	0.4 ± 0.03	0.9 ± 0.08
k_{cat}[b,c] (s^{-1})	69 ± 7	2760 ± 31	1012 ± 11
k_{cat}/K_M(ABTS) (mM^{-1} s^{-1})	53	6900	1124
$K_M(H_2O_2)$[c] (mM)	2.8 ± 0.4	0.52 ± 0.06	2 ± 0.015
$k_{cat}/K_M(H_2O_2)$ (mM^{-1} s^{-1})	25	5300	506

[a] Buffer used: 100 mM MOPS, pH 6.5. [b] Using saturating concentrations of H_2O_2 (25 mM). [c] Using saturating concentrations of ABTS (10 mM). [d] $[Ca^{2+}]$ = 10 mM. [e] $[Ca^{2+}]$ = 0.2 mM.

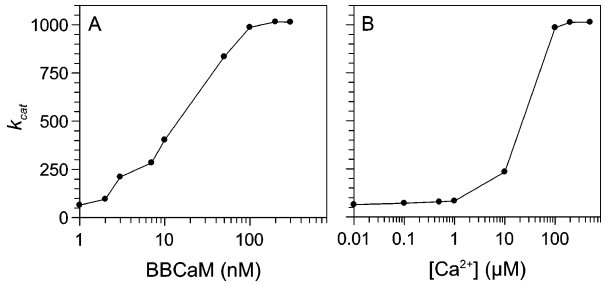

FIGURE 8: Response of *Euphorbia* peroxidase activity to Ca^{2+}/BBCaM. ELP activity in response to increasing BBCaM concentrations in the presence of 0.2 mM calcium ions (A). ELP activity in response to increasing free calcium concentrations in the presence of 0.3 μM BBCaM (B). Buffer: 100 mM MOPS, pH 6.5.

Organization of ELP and ELCaM in the Euphorbia Genome. To determine the organization of either the ELP and the ELCaM gene in the *E. characias* genome, full chromosomal DNA was digested with *Eco*RI, *Hin*dIII, and

```
Euphorbia       MADQLTDDQISEFKEAFSLFDKDGDGCITTKELGTVMRSLGQNPTEAELQDMINEVDADG  60
Bos taurus      -ADQLTEEQIAEFKEAFSLFDKDGDGTITTKELGTVMRSLGQNPTEAELQDMINEVDADG  59

Euphorbia       NGTIDFPEFLNLMARKMKDTDSEEELKEAFRVFDKDQNGFISAAELRHVMTNLGEKLTDE 120
Bos taurus      NGTIDFPEFLTMMARKMKDTDSEEEIREAFRVFDKDGNGYISAAELRHVMTNLGEKLTDE 119

Euphorbia       EVDEMIREADVDGDGQINYEEFVKVMMAK 149
Bos taurus      EVDEMIREADIDGDGQVNYEEFVQMMTAK 148
```

FIGURE 7: Sequence comparison of *E. characias* CaM and *Bos taurus* (bovine) brain CaM. Conserved residues are in gray. Dashes indicate gaps in alignment. ELCaM shares ≈90% sequence identity with BBCaM (GenBank accession number AB099053).

Table 2: Kinetic Parameters of *Euphorbia* Latex Peroxidase (ELP) and Horseradish Peroxidase (HRP) in the Presence and Absence of Ca^{2+} Ions and Bovine Brain Calmodulin (BBCaM)[a]

peroxidase	k_{cat} (s^{-1})[b]
ELP	69 ± 7
ELP + Ca^{2+} (0.2 mM)	125 ± 14
ELP + Ca^{2+} (10 mM)	2760 ± 31
ELP + BBCaM	65 ± 8
ELP + Ca^{2+} (0.2 mM) + BBCaM (10 nM)	430 ± 10
ELP + Ca^{2+} (10 mM) + BBCaM (10 nM)	2800 ± 25
ELP + Ca^{2+} (0.2 mM) + BBCaM (0.3 μM)	1012 ± 11
ELP + Ca^{2+} (10 mM) + BBCaM (0.3 μM)	2790 ± 33
HRP	880 ± 98
HRP + Ca^{2+} (0.2 mM)	870 ± 95
HRP + Ca^{2+} (10 mM)	890 ± 71
HRP + BBCaM	890 ± 92
HRP + Ca^{2+} (0.2 mM) + BBCaM (0.3 μM)	880 ± 70
HRP + Ca^{2+} (10 mM) + BBCaM (0.3 μM)	870 ± 90

[a] Peroxidase (6×10^{-4} μM) activity was measured at 25 °C using saturating concentrations of ABTS (10 mM) as reducing substrate and saturating concentrations of H_2O_2 (25 mM) in 100 mM MOPS buffer, pH 6.5. [b] k_{cat} is defined as moles of substrate consumed per mole of active sites per second. Values are ±SEM from three independent measurements.

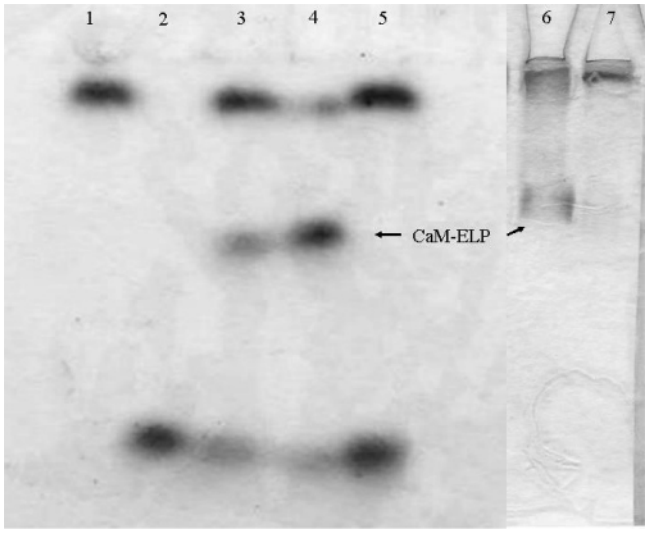

FIGURE 9: Native PAGE and activity staining of purified ELP in the presence of BBCaM and calcium ions. Lanes: 1, ELP (0.1 μM); 2, BBCaM (0.6 μM); 3, ELP (0.1 μM) incubated with BBCaM (0.3 μM) in the presence of 300 μM calcium ions; 4, ELP (0.1 μM) incubated with BBCaM (0.6 μM) in the presence of calcium ions (300 μM); 5, as in lane 4 but in the absence of calcium ions; 6, staining for ELP activity in the presence of BBCaM and Ca^{2+} (see lane 3); the gel was first stained with Coomassie blue, and then protein bands with peroxidase activity were detected by incubating the gel in a buffer containing *o*-dianisidine and hydrogen peroxide; 7, staining for ELP activity in the absence of BBCaM and Ca^{2+} (see lane 1).

*Bam*HI, and the filter membrane was hybridized with full-length *Euphorbia* ELP or ELCaM cDNA as a probe. *Eco*RI and *Bam*HI digestions revealed one major band, whereas *Hin*dIII digestion gave three bands as expected, since two *Hin*dIII restriction sites are present in the cDNA clones (results not shown). These results indicate that the *E. characias* genome contains a single peroxidase and a single CaM gene. RT-PCR experiments coupled with northern blot and cDNA blot analysis revealed in concert that homogeneous calmodulin and peroxidase mRNA population occurs in leaf tissue as in latex and that alternative splicing does not occur (data not shown).

DISCUSSION

In recent years, evidence has grown that plant defense systems rely in part on a finely regulated cross-talk between calcium and H_2O_2 (*19*, *20*, *39*−*42*). Abiotic elicitors and pathogens trigger a rapid accumulation of cytosolic Ca^{2+} deriving from both extracellular compartments and intracellular stores. Released calcium may activate the plasma membrane NADPH-dependent oxidase complex, the main enzymatic machinery responsible for the production of H_2O_2 and other ROS in plants. Regulation of the NADPH oxidase complex by calcium may occur either directly thanks to the affinity of the protein for the metal ion or indirectly by elevating the concentration of available NADPH via modulation of the activity of NAD kinase, a CaM-dependent enzyme that catalyzes the final step in the production of NADPH. After production, H_2O_2 and other ROS fuel a rapid, transient, and nonspecific oxidative burst to contrast pathogens at the site of infection. ROS are also detected by specific receptors and an associated transduction pathway that again involves Ca^{2+} and Ca^{2+}-binding proteins among other players and ultimately results in the activation of specific and prolonged cellular defense responses (*19*). Another important downstream target of H_2O_2 and ROS is the activation of Ca^{2+}-permeable channels in plant membranes, which boosts calcium influx and further stimulates H_2O_2 generation by NADPH oxidase (*41*, *42*). Since the correct functioning of H_2O_2 and ROS signaling depends not only by production but also by scavenging, a number of enzymes are at work to remove ROS, thus controlling the duration and intensity of signals and maintaining a correct low steady-state level of H_2O_2 and cognate oxygen species (*19*). As far as calcium is concerned, recent findings indicate that at least one component of the plant ROS-scavenging apparatus, namely, catalase, which catalyzes the degradation of H_2O_2 into water and oxygen, is regulated by Ca^{2+}/CaM (*20*).

From what is briefly outlined above, it is apparent that calcium has a dual role in regulating H_2O_2/ROS homeostasis and signaling in plants, acting as both a positive and negative modulator, and that CaM is a recurrent transducer of Ca^{2+} signals along these pathways. Here we add a significant element to this scenario, demonstrating for the first time that a plant peroxidase is Ca^{2+}/CaM-regulated and might participate to the control of H_2O_2/ROS levels and activity in plant defense responses. Peroxidases can contribute to the H_2O_2-scavenging capacity of plants by using a range of reductants, removing the H_2O_2 generated by the NAPDH complex, but also by other enzymatic systems such as xanthine oxidase, amine oxidase, and germin-like oxidase, in addition to that produced by normal metabolism in chloroplasts, mitochondria, and peroxisomes (*19*, *21*). On the other side, plant peroxidases have the potential to produce H_2O_2 on their own. This is well-known for cell wall peroxidases, for which H_2O_2 production was shown to be strongly pH-dependent, with a maximum at neutral to basic pH, and to be stimulated by plant−pathogen interactions in several instances (*43*). The peroxidase-generated H_2O_2 contributes to the oxidative burst deployed by the plant in response to attack or injury, enters ROS signaling, and might also trigger the cross-linking of proteins and phenolics to

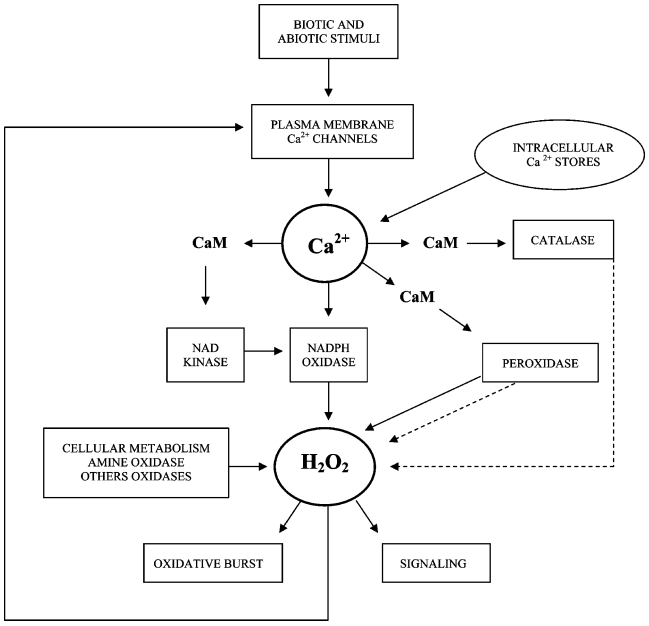

FIGURE 10: Generalized model of the Ca^{2+}−hydrogen peroxide cross-talk in plant defense reactions. A variety of biotic and abiotic stresses may elicit the transient increase of cytosolic Ca^{2+} levels by modulating the opening of plasma membrane Ca^{2+}-permeable cation channels. Calcium ions might also be released from intracellular stores, such as vacuoles. Calcium stimulates the production of H_2O_2, mainly by activating the NADPH oxidase complex either via direct binding or through a Ca^{2+}/CaM-regulated NAD kinase. Ca^{2+}/CaM-binding peroxidase might be another important source of H_2O_2, and this is also generated in normal cellular metabolism and by amine oxidases and other oxidative enzymes. Scavenging of H_2O_2 is mediated by a complex network of enzymes, including the Ca^{2+}/CaM-regulated catalase and peroxidase. A rapid and transient production of high levels of H_2O_2 and other ROS causes an oxidative burst as the early defense reaction. At the same time, H_2O_2 acts as a signaling molecule, and the associated signal transduction pathway regulates systemic and long-lasting defense responses and other biological processes. H_2O_2 also activates plasma membrane Ca^{2+} channels, stimulating further H_2O_2 production. Solid lines mark positive regulations and dashed lines negative ones.

reinforce cell walls at the site of infection, which would conceivably result in suppression of pathogen ingress (*43*, *44*). On the basis of the results reported here, we therefore propose a model of the interplay between Ca^{2+} and H_2O_2 signaling pathways in plant defense that envisages peroxidase as an important point of transduction of calcium signals and control of H_2O_2 homeostasis, contributing to both the positive and negative regulation of its levels (Figure 10).

Euphorbia Peroxidase and Euphorbia Calmodulin: Associated Enzymes Always or Sometimes? Although the scheme depicted in Figure 10 may well be of general validity, it remains somehow hypothetical in the context of laticifers and their content. ELP shows a signal peptide typical of secreted proteins whereas ELCaM does not. This may indicate that while ELP is excreted in the latex, calmodulin resides into the cytosol, and under normal conditions ELP activity is only modulated by calcium ions. To account in vivo for the in vitro observed modulation of ELP activity by Ca^{2+}/CaM, one could hypothesize that, following plant injury and tissue rupture, latex and cytoplasm content mix, so that CaM can interact with ELP and stimulate its activity, boosting the production of H_2O_2, fueling oxidative burst and H_2O_2 signaling with associated defense responses against invading pathogens and environmental stresses.

Another, more distant, possibility is offered by the analysis of the ELCaM sequence, which shows the presence of the tyrosine-based sorting signal YxxΦ (Φ, bulky hydrophobic residue) described in various proteins destined to be internalized by clathrin pathways (*45*). In theory, the ELCaM peptide ^{139}YEEF^{142} could be recognized by the μ1 subunit of the heterotetrameric adaptor protein AP1, the derived complex being then anchored to the vacuole membrane through clathrin (*46*). The formation of the ELCaM−ELP complex would thus be explained in this case by assuming that a clathrin-mediated internalization mechanism is in force which is able to mediate the uptake of ELCaM into the vacuole.

An interesting point to be addressed by future studies is whether ELP is activated by Ca^{2+}/CaM and free Ca^{2+} in similar or different ways, i.e., if Ca^{2+}/CaM binding to ELP provokes the saturation of the distal calcium-binding site and the subsequent protein rearrangement seen following ELP exposure to excess free calcium, or if the mechanism of CaM-mediated regulation follows another route. Intriguingly, in the predicted structure of heme pocket and calcium-binding sites, the heme distal His_{50} is in contact with Asn_{78}, which in turn flanks the CaM-binding 1-8-14 peptide. Moreover, very little information is available about Ca^{2+} signaling and H_2O_2 cycling in *Euphorbia* latex and on the associated enzymes. The only characterized system, besides ELP, is the H_2O_2-producing *Euphorbia* latex amine oxidase (*47*). Plant amine oxidases are copper/quinone-containing enzymes that catalyze the oxidative deamination of diamines and polyamines to aldehydes and ammonia, concomitantly with a two-electron reduction of dioxygen to hydrogen peroxide (*48*). Although the exact physiological role of plant amine oxidases is unknown, they are believed to be implicated in the synthesis and/or degradation of secondary metabolites and to participate to the lignification of cell wall and to oxidative burst through the production of H_2O_2 (*19*, *48*, *49*). Clearly, additional research is needed to explore the exact localization of peroxidase and calmodulin at both the cell and whole plant levels in *Euphorbia* and the functional interactions of ELP with amine oxidase and other latex enzymatic systems and to understand the latex role in plant defense.

SUPPORTING INFORMATION AVAILABLE

Comparison of the deduced amino acid sequence of *E. characias* peroxidase with other peroxidases from plants and comparison of the deduced amino acid sequence of *E. characias* CaM with other CaMs from plants. This material is available free of charge via the Internet at http://pubs.acs.org.

REFERENCES

1. Medda, R., Padiglia, A., Longu, S., Bellelli, A., Arcovito, A., Cavallo, S., Pedersen, J. Z., and Floris, G. (2003) Critical role of Ca^{2+} ions in the reaction mechanism of *Euphorbia characias* peroxidase, *Biochemistry 42*, 8909−8918.
2. Reddy, A. S. N. (2001) Calcium: silver bullet in signaling, *Plant Sci. 160*, 381−404.
3. Reddy, V. S., Ali, G. S., and Reddy, A. S. N. (2002) Genes encoding calmodulin-binding proteins in the *Arabidopsis* genome, *J. Biol. Chem. 277*, 9840−9852.
4. Harper, J. F., Breton, G., and Harmon, A. (2004) Decoding Ca^{2+} signals through plant protein kinases, *Annu. Rev. Plant Biol. 55*, 263−288.

5. Anderson, J. M., Charbonneau, H., Jones, H. P., McCann, R. O., and Cormier, M. J. (1980) Characterization of the plant nicotinamide adenine dinucleotide kinase activator protein and its identification as calmodulin, *Biochemistry 19*, 3113−3120.
6. Snedden, W. A., and Fromm, H. (2001) Calmodulin as a versatile calcium signal transducer in plants, *New Phytol. 151*, 35−66.
7. Moutinho, A., Love, J., Trewavas, A. J., and Malho, R. (1998) Distribution of calmodulin protein and mRNA in growing pollen tubes, *Sex Plant Reprod. 11*, 131−139.
8. Golovkin, M., and Reddy, A. S. N. (2003) A calmodulin-binding protein from *Arabidopsis* has an essential role in pollen germination, *Proc. Natl. Acad. Sci. U.S.A. 100*, 10558−10563.
9. Hua, W., Zhang, L., Liang, S. P., Jones, R. L., and Lu, Y. T. (2004) A tobacco calcium/calmodulin-binding protein kinase functions as a negative regulator of flowering, *J. Biol. Chem. 279*, 31483−31494.
10. Hua, W., Li, R. J., Wang, L., and Lu, Y. T. (2004) A tobacco calmodulin-binding protein kinase (*NtCBK2*) induced by high-salt/GA treatment and its expression during floral development and embryogenesis, *Plant Sci. 166*, 1253−1259.
11. Kim, C. M., Lee, S. H., Kim, J. K., Chun, H. J., Choi, M. S., Chung, W. S., Moon, B. C., Kang, C. H., Park, C. Y., Yoo, J. H., Kang, Y. H., Koo, S. C., Koo, Y. D., Jung, J. C., Kim, S. T., Schulze-Lefert, P., Lee, S. Y., and Cho, M. J. (2002) Mlo, a modulator of plant defense and cell death, is a novel calmodulin-binding protein. Isolation and characterization of a rice Mlo homologue, *J. Biol. Chem. 277*, 19304−19314
12. Zielinski, R. E. (1998) Calmodulin and calmodulin-binding proteins in plants, *Annu. Rev. Plant Physiol. Plant Mol. Biol. 49*, 697−725.
13. Yang, T., and Poovaiah, B. W. (2003) Calcium/calmodulin-mediated signal network in plants, *Trends Plant Sci. 8*, 505−512.
14. Zhang, L., and Lu, Y. T. (2003) Calmodulin-binding protein kinases in plants, *Trends Plant Sci. 8*, 123−127.
15. Hiraga, S., Sasaki, K., Ito, H., Ohashi, Y., and Matsui, H. (2001) A large family of Class III plant peroxidases, *Plant Cell Physiol. 42*, 462−468.
16. Klessig, D. F., Durner, J., Noad, R., Navarre, D. A., Wendehenne, D., Kumar, D., Zhou, J. M., Shah, J., Zhang, S., Kachroo, P., Trifa, Y., Pontier, D., Lam, E., and Silva, H. (2000) Nitric oxide and salicylic acid signaling in plant defense, *Proc. Natl. Acad. Sci. U.S.A. 97*, 8849−8855.
17. Kawano, T. (2003) Roles of the reactive oxygen species-generating peroxidase reactions in plant defense and growth induction, *Plant Cell. Rep. 21*, 829−837.
18. Orozco-Cardenas, M. L., Narvaez-Vasquez, J., and Ryan, C. A. (2001) Hydrogen peroxide acts as a second messenger for the induction of defense genes in tomato plants in response to wounding, systemin, and methyl jasmonate, *Plant Cell 13*, 179−191.
19. Mittler, R., Vanderauwera, S., Gollery, M., and Van Breusegem, F. (2004) The reactive oxygen gene network of plants, *Trends Plant Sci. 9*, 490−498.
20. Yang, T., and Poovaiah, B. W. (2002) Hydrogen peroxide homeostasis: activation of plant catalase by calcium/calmodulina, *Proc. Natl. Acad. Sci. U.S.A. 99*, 4097−4102.
21. Neill, S., Desikan, R., and Hancock, J. (2002) Hydrogen peroxide signaling, *Curr. Opin. Plant Biol. 5*, 388−395.
22. Rudall, P. (1994) Lactifers in Crotonoideae (Euphorbiaceae): homology and evolution, *Ann. MO Bot. Gard. 81*, 270−282.
23. Webster, G. L. (1994) Classification of the Euphorbiaceae, *Ann. MO Bot. Gard. 81*, 3−32.
24. Ko, J. H., Chow, K. S., and Han, K. H. (2003) Transcriptome analysis reveals novel features of the molecular events occurring in the laticifers of *Hevea brasiliensis* (para rubber tree), *Plant Mol. Biol. 53*, 479−492.
25. Kekwick, R. G. O. (2001) *Latex and Laticifers Encyclopedia of Life Sciences*, http://www.els.net.
26. Furhop, J. H., and Smith, K. M. (1975) Laboratory methods in *Porphyrins and metalloproteins* (Smith, K. M., Ed.) pp 757−869, Elsevier, Amsterdam.
27. Rose, T. M., Henikoff, J. G., and Henikoff, S. (2003) CODEHOP (COnsensus-DEgenerate Hybrid Oligonucleotide Primer) PCR primer design, *Nucleic Acids Res. 31*, 3763−3766.
28. Frohman, M. A. (1993) Rapid amplification of complementary DNA ends for generation of full-length complementary DNAs: thermal RACE, *Methods Enzymol. 218*, 340−356.
29. Jaakola, L., Pirttilä, A. M., and Hohtola, A. (2001) cDNA blotting offers an alternative method for gene expression studies, *Plant Mol. Biol. Rep. 19*, 125−128.
30. Howes, B. D., Feis, A., Raimondi, L., Indiani, C., and Smulevich, G. (2001) The critical role of the proximal calcium ion in the structural properties of horseradish peroxidase, *J. Biol. Chem. 276*, 40704−40711.
31. Laberge, M., Huang, Q., Schweitzer-Stenner, R., and Fidy, J. (2003) The endogenous calcium ions of horseradish peroxidase C are required to maintain the functional nonplanarity of the heme, *Biophys. J. 84*, 2542−2552.
32. Yap, K. L., Kim, J., Truong, K., Sherman, M., Yuan, T., and Ikura, M. (2000) Calmodulin target database, *J. Struct. Funct. Genomics 1*, 8−14.
33. Houdusse, A., and Cohen, C. (1995) Target sequence recognition by the calmodulin superfamily: Implications from light chain binding to the regulatory domain of scallop myosin, *Proc. Natl. Acad. Sci. U.S.A. 92*, 10644−10647.
34. Munshi, H. G., Burks, D. J., Joyal, J. L., White, M. F., and Sacks, D. B. (1996) Ca^{2+} regulates calmodulin binding to IQ motifs in IRS-1, *Biochemistry 35*, 15883−15889.
35. Bähler, M., and Rhoads, A. (2002) Calmodulin signaling via the IQ motif, *FEBS Lett. 513*, 107−113.
36. Putkey, J. A., Kleerekoper, Q., Gaertner, T. R., and Waxham, M. N. (2003) A new role for IQ motif proteins in regulating calmodulin function, *J. Biol. Chem. 278*, 49667−49670.
37. Rhoads, A. R., and Friedberg, F. (1997) Sequence motifs for calmodulin recognition, *FASEB J. 11*, 331−340.
38. Erickson-Viitanen, S., and DeGrado, W. F. (1987) Recognition and characterization of calmodulin-binding sequences, *Methods Enzymol. 139*, 455−478.
39. Grant, J. J., and Loake, G. J. (2000) Role of active oxygen intermediates and cognate redox signaling in disease resistance, *Plant Physiol. 124*, 21−29.
40. Pellinen, R. I., Korhonen, M. S., Tauriainen, A. A., Palva, E. T., and Kangasjärvi, J. (2002) Hydrogen peroxide activates cell death and defense gene expression in birch, *Plant Physiol. 130*, 549−560.
41. Demidchik, V., Shabala, S. N., Coutts, K. B., Tester, M. A., and Davies, J. M. (2002) Free oxygen radicals regulate plasma membrane Ca^{2+} and K^{+}-permeable channels in plant root cells, *J. Cell Sci. 116*, 81−88.
42. Foreman, J., Demidchik, V., Bothwell, J. H., Mylona, P., Miedema, H., Torres, M. A., Linstead, P., Costa, S., Brownlee, C., Jones, J. D., Davies, J. M., and Dolan, L. (2003) Reactive oxygen species produced by NADPH oxidase regulate plant cell growth, *Nature 422*, 442−446.
43. Bolwell, G. P., and Wojtaszek, P. (1997) Mechanisms for the generation of active oxygen species in plant defence: a broad perspective, *Physiol. Mol. Plant Pathol. 51*, 347−366.
44. Wu, G., Shortt, B. J., Lawrence, E. B., León, J., Fitzsimmons, K. C., Levine, E. B., Raskin, I., and Shah, D. M. (1997) Activation of host defense mechanisms by elevated production of H_2O_2 in transgenic plants, *Plant Physiol. 115*, 427−435.
45. Ohno, H., Stewart, J., Fournier, M. C., Bosshart, H., Rhee, I., Miyatake, S., Saito, T., Gallusser, A., Kirchhausen, T., and Bonifacino, J. S. (1995) Interaction of tyrosine-based sorting signals with clathrin-associated proteins, *Science 269*, 1872−1875.
46. Brett, T. J., Traub, L. M., and Fremont, D. H. (2002) Accessory protein recruitment motifs in clathrin-mediated endocytosis, *Structure 10*, 797−809.
47. Padiglia, A., Medda, R., Lorrai, A., Murgia, B., Pedersen, J. Z., Finazzi Agrò, A., and Floris, G. (1998) Characterization of *Euphorbia characias* latex amine oxidase, *Plant Physiol. 117*, 1363−1371.
48. Medda, R., Padiglia, A., and Floris, G. (1995) Plant copper-amine oxidases, *Phytochemistry 39*, 1−9.
49. Laurenzi, M., Tipping, A. J., Marcus, S. E., Knox, J. P., Federico, R., Angelini, R., and McPherson, M. J. (2001) Analysis of the distribution of copper amine oxidase in cell walls of legume seedlings, *Planta 214*, 37−45.
50. Kyte, J., and Doolittle, R. F. (1982) A simple method for displaying the hydropathic character of a protein, *J. Mol. Biol. 157*, 105−132.
51. Chou, P. Y., and Fasman, G. D. (1978) Empirical predictions of protein conformation, *Annu. Rev. Biochem. 47*, 251−276.

BI0513251